Journal of Food Engineering 392 (2025) 112470

Contents lists available at ScienceDirect

Journal of Food Engineering

journal homepage: www.elsevier.com/locate/jfoodeng

Non-invasive textural assessment of puffed corn cakes using air-coupled ultrasound

Virginia Sanchez-Jimenez [a], Lola Fariñas [a,b], Anabella S. Giacomozzi [a], Alba Ginel [b], Amparo Quiles-Chuliá [a], Tomas E. Gomez Alvarez-Arenas [b], Jose Benedito [a], Jose V. Garcia-Perez [a,*]

[a] Institute of Food Engineering FoodUPV, Universitat Politécnica de València, Camí de Vera s/n, Edificio 3F, Valencia, 46022, Spain
[b] Institute of Physical and Information Technologies (ITEFI), CSIC, Serrano 144, 28006, Madrid, Spain

ARTICLE INFO

Keywords:
Air-coupled ultrasound
Texture
Moisture adsorption
Attenuation
Non-destructive

ABSTRACT

This study aimed to evaluate the feasibility of using air-coupled ultrasound for the textural characterization of puffed corn cakes (PCC). For this purpose, air-coupled ultrasound measurements (0.15–0.4 MHz) were taken and instrumental texture, microstructural (Cryo-FESEM), moisture content and water activity analyses were performed on two different sets of PCC: 1) Seven commercial batches and 2) Four commercial batches stored at different relative humidities (10–40 %) in order to provoke slight changes in moisture content.

The variation in the transmission coefficient modulus with the frequency (ΔCT_f, dB/MHz) was the ultrasonic parameter chosen due to fact that the jagged surface of the PCC hindered an accurate estimation of the ultrasound velocity. Thus, ΔCT_f was able to explain the PCC viscoelastic behaviour and correlated significantly ($p < 0.05$) with the PCC apparent hardness ($R^2 = 0.89$) for every batch analyzed. ΔCT_f also permitted the computation of the increase in attenuation due to microstructural changes brought about by moisture adsorption.

1. Introduction

Texture is one of the main quality parameters during the production and shelf-life of extruded cereal snacks, influenced by both composition and manufacturing conditions. The loss of crispness in dry snacks leads to consumer rejection of these products (Jakubczyk et al., 2008a,b; Jiang et al., 2021). Moisture excess during production or moisture adsorption during storage could be two reasons for the reduced quality of extruded snacks (Sanchez-Jimenez et al., 2022; Wani and Kumar, 2016). Depending on the moisture content and adsorption conditions, a hardening (anti-plasticizing effect) or softening (plasticizing effect) of the product could be the main changes related to the loss in the desired degree of crispness.

Puffed corn cakes (PCC) are extruded cereal products and the fact that they are a healthy snack which is also easy to transport has led to a notable increase in consumer demand in recent years (Sanchez-Jimenez et al., 2022; Sharma, 2012; Wani and Kumar, 2016). However, the complex structure of PCC makes it challenging to perform quality control, which is necessary to ensure optimal sensory characteristics. PCC are defined as a solid foam-like product with an internal network of cavities and a jagged surface that complicates a textural analysis. Previous studies characterized the texture of puffed cakes at laboratory scale by means of flexion (Lewicki and Jakubczyk, 2004), compression (Laurindo and Peleg, 2007) and hybrid flexion-compression tests (Sanchez-Jimenez et al., 2022). However, these studies showed that there were several challenges in terms of the standardization of the instrumental texture analysis of this product for routine industrial quality control: i) a considerable sample size is required due to its highly variable nature, ii) specific texture probes and measurement conditions adapted to the rough and irregular surface are necessary and iii) measurements are time-consuming and destructive, making it unsuitable for the evaluation of the entire production in online systems. These issues have driven the search for new methods towards industrial digitalization. Thus, the introduction of sensors in the PCC production lines for real-time, non-destructive and non-invasive monitoring represents a significant challenge for this industry (Elfawakhry et al., 2013; Hassoun et al., 2023).

Ultrasound (US) is widely used as a form of non-destructive testing (NDT) in the medical, metallurgic, civil engineering, aerospace and aeronautic sectors and has great potential for application in the food

* Corresponding author.
E-mail address: jogarpe4@tal.upv.es (J.V. Garcia-Perez).

https://doi.org/10.1016/j.jfoodeng.2025.112470
Received 1 October 2024; Received in revised form 7 January 2025; Accepted 8 January 2025
Available online 13 January 2025

industry (Awad et al., 2012; Elfawakhry et al., 2013; Mohd Khairi et al., 2016). The propagation of the ultrasonic waves is heavily influenced by the mechanical properties of the food matrix through which they travel, causing modifications in the ultrasonic parameters, such as velocity or attenuation. This represents a distinguishing factor for ultrasonic techniques compared to other non-destructive technologies, such as photonic ones, which are more sensitive to molecular aspects than to textural or structural properties. Thus, US parameters have been well correlated with the quality properties of a wide range of food products, such as the firmness of apples (Vasighi-Shojae et al., 2018), the salt gain and moisture loss during dry-cured ham salting (Contreras et al., 2021), the density of oranges (Morrison and Abeyratne, 2014), and the mechanical properties of honey (González-Mohino et al., 2019) and wheat noodle dough (Strybulevych et al., 2019). However, most of the previous studies have applied the contact US technique, which needs the coupling of the transducers to the sample surface to ensure an efficient wave transmission (Fariñas et al., 2021a; Sanchez-Jimenez et al., 2023). This requirement limits the adoption of US testing techniques in the food industry and, specifically, in the cereal snack production. The porous, jagged and fragile structure that characterizes the extruded cereal snacks, such as PCC, makes the use of contact techniques unsuitable. For that reason, the ultrasonic inspection of PCC, and other snacks, must be addressed using air-coupled or contactless ultrasound. This approach offers several advantages at an industrial level including easy installation, moderate cost and fast measurement (Elfawakhry et al., 2013; Fariñas et al., 2021a). The advantages of contactless US for food quality control purposes were first reported by Gan et al. (2002, 2006) to inspect packaged products and monitor the coagulation of milk, respectively. More recently, Kerhervé et al. (2019) studied the feasibility of online US measurement for the industrial quality control of noodle dough according to the moisture content, and Fariñas et al. (2021b) assessed the post-harvest textural modification of avocado during ripening. However, to our knowledge, the monitoring of the quality traits of extruded snacks has not previously been addressed. Therefore, the present study aims to determine the feasibility of air-coupled US for two purposes: i) to characterize the textural properties of commercial PCC batches and ii) to detect variations in these properties due to moisture adsorption during storage. This could be of great interest in addressing an industrial-level challenge and is closely aligned with the Sustainable Development Goals in the current digital context.

2. Materials and methods

2.1. Raw sample

Commercial PCC were supplied by Cerealto Group (Venta de Baños, Spain). The samples (9.2 mm of diameter) were kept in their original package and stored at room temperature (22 ± 1 °C) until the experimental analysis was carried out. Two different PCC sets were analyzed: i) Seven batches manufactured on different days (Set 1, Fig. 1) (N = 210, 30 per batch) and ii) A PCC set split into 5 batches, one of which is used as control and four stored at different relative humidity (RH) in order to induce minor changes in moisture content (N = 150, 30 per batch) (Set 2, Fig. 1). The choice of Set 1 aimed to show the natural experimental variability on PCC texture linked to raw materials and manufacturing conditions. While from Set 2, the influence of slight changes of moisture content on PCC texture was analyzed.

2.2. Storage at different RH for moisture adsorption

PCC storage (Set 2) was carried out according to the experimental methodology reported by Sanchez-Jimenez et al. (2022). Different saturated salt solutions were placed inside hermetic glass containers to keep the RH constant during storage, in the range of 10–40 % (10 %, LiCl; 20 %, CH_3COOK; 30 %, $MgCl_2$; 40 %, K_2CO_3). Thus, PCC were stored at different RH and at room temperature (22 ± 2 °C) for 15 days. Storage time was established by a preliminary test, weighing the samples every two days to monitor the moisture adsorption.

2.3. Moisture content and water activity analysis

The moisture content (W) of PCC was determined by a gravimetric method (AOAC, 1997; method 934.06), drying the samples in a convection oven at 105 °C until the equilibrium weight was reached. W was

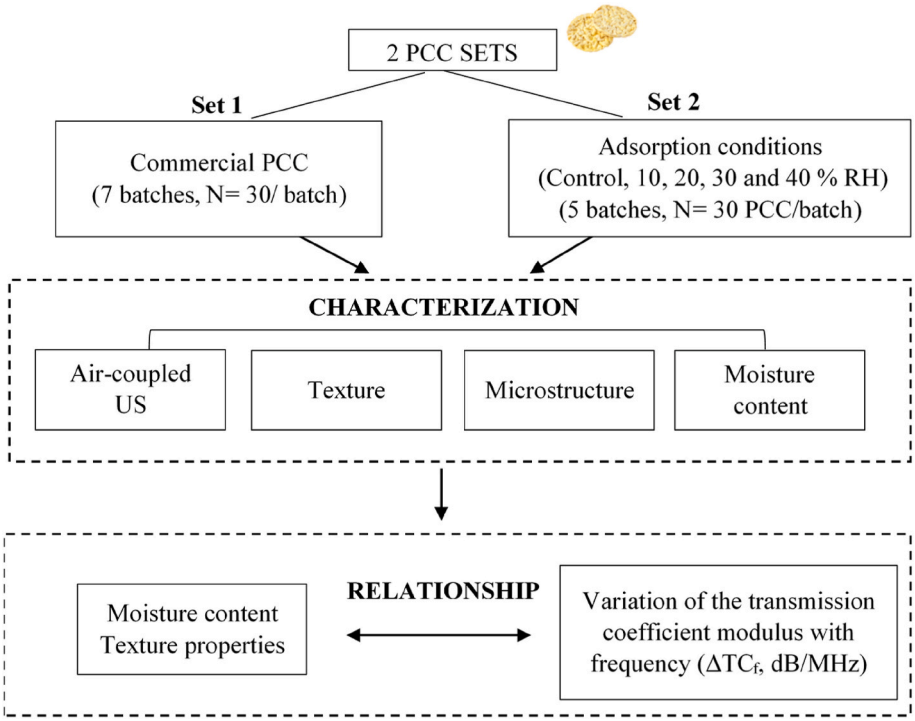

Fig. 1. Working plan for analysis of Puffed Corn Cakes (PCC).

expressed as kg water (w)/kg dry matter (dm). Water activity (a_w) was measured at 23 °C using a dew-point hygrometer (Sprint th 500, Novasina AG, Switzerland). Both experimental analyses were carried out with the samples homogenized using a household electrical grinder (Blixer 2, Robot Coupe®, France). Each analysis was carried out in triplicate for every batch of PCC.

2.4. Ultrasonic measurements

The air-coupled ultrasonic experimental set-up consisted of a pair of unfocused piezoelectric transducers specifically designed for efficient ultrasonic signal propagation through the air (Ginel and Alvarez-Arenas, 2019; Kelly et al., 2001). The transducers have a central frequency of 280 kHz, a bandwidth of 0.15–0.40 MHz, a peak sensitivity of −25 dB, an electrical impedance in transmission mode of about 100 Ω, and a circular aperture with a diameter of 25 mm. The estimation of the useable bandwidth of these transducers is obtained by the −20 dB band, this is not the conventional bandwidth figure used for water immersion transducers, but this is a more significant figure to reveal the actual frequency band where transducers can be used (Ginel and Alvarez-Arenas, 2019). A pulser-receiver (5077 PR, Olympus, Houston, TX, USA) was used to drive the transmitter transducer with a 400 V semi-cycle of square wave tuned to the transmitter transducer. Then, the signal acquired by the receiver transducer was filtered using the built-in Low Pass Filter with a 10 MHz cut-off frequency and amplified (59 dB) at its reception. An oscilloscope (MDO3024, Tektronix, WA, USA), digitalized (10 MS/s) and averaged (128 signals) the signals to reduce signal-to-noise ratio. Finally, the signals were stored and analyzed using Python software (pyVISA, Numpy and Matplotlib) in a PC. Measurements were taken in through-transmission mode with the transmitter and receiver transducers perfectly aligned at a distance of 10 cm from each other. Reducing the distance between transducers, up to a minimum separation of 2 cm, would decrease air attenuation and increase Signal-to-Noise Ratio in laboratory measurements. However, this approach would hinder the extrapolation of the experimental results to industrial applications, as such environments typically require greater distances for the feasible placement of sensors along processing lines, which justifies the choice of 10 cm for the transducers' separation. A platform with a hole (22 mm diameter) was placed between both transducers to easily position and measure the samples. The diameter hole has to be chosen in order to avoid any kind of distortion on the ultrasonic signal path and forcing it to travel through the sample. Firstly, the reference signal travelling through the air (without sample) was recorded for calibration immediately before each PCC was measured. Afterward, the PCC was positioned on the platform and up to 7 measurements were taken at different points. The measurements were distributed to ensure a thorough analysis of the PCC surface by sliding the cake and avoiding the edges.

The analysis of the signals was conditioned by the jagged and irregular surface of the PCC. The irregularity of the surface led to considerable variability in the waveform of the signals and the first wavefront arrival or time-of-flight (TOF), even within the same PCC, as shown in Fig. 2A. This, together with the difficulty in measuring effective PCC thickness, hampered an accurate calculation of ultrasonic velocity. Therefore, the ultrasonic analysis focused on the spectral response. The Fast Fourier Transform (FFT) was applied to the signals in the time domain and the transmission coefficient spectra (TC) were computed (Eq. (1)) and averaged for each cake (7 measurement points). The variation of the transmission coefficient modulus (ΔTC_f, dB/MHz) represents the derivative of TC with respect to frequency (Eq. (2)). In the present work, TC followed a linear pattern with the frequency within the transducers' bandwidth (Fig. 2B) thus, ΔTC_f was calculated from the slope of this linear relationship. ΔTC_f is related to the PCC attenuation (the lower the ΔTC_f, the larger the attenuation) and is non-dependent on the PCC thickness (Sanchez-Jimenez et al., 2023).

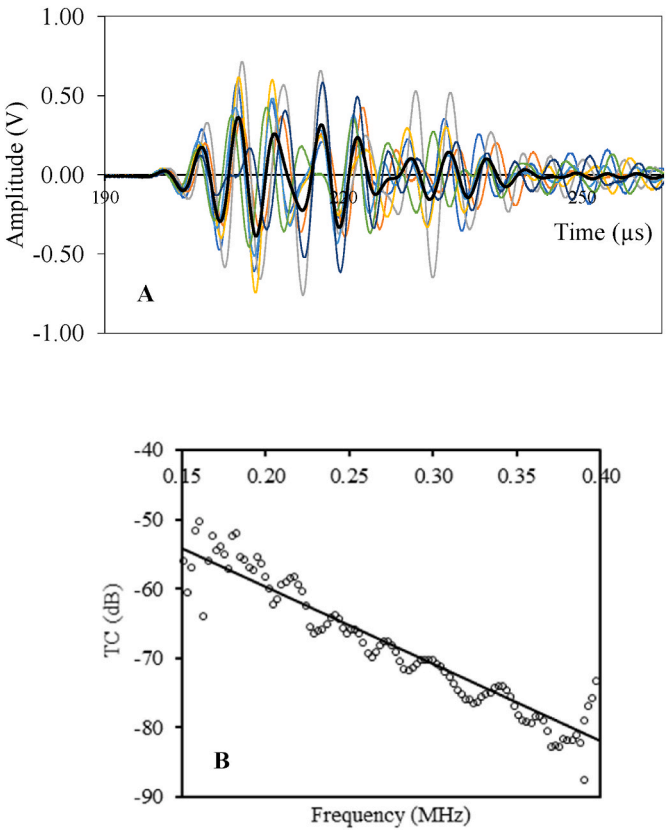

Fig. 2. A) Ultrasonic signal replicates (N = 7) acquired (0.28 MHz) in the same puffed corn cake (PCC) (coloured line) and averaged signal (black line); B) Average (N = 7) spectrum of the transmission coefficient (TC, dB). The solid line represents the linear relationship between the transmission coefficient (TC) and frequency within the transducers' bandwidth (0.15–0.40 MHz).

$$TC = 20 \log\left(\frac{A}{A_0}\right) \quad \text{Eq. 1}$$

Where A and A_0 are the amplitudes for each frequency of the frequency spectrum for the PCC and reference signals, respectively.

$$\Delta TC_f = \frac{dTC}{df} \quad \text{Eq. 2}$$

Where f denotes the frequency (MHz).

2.5. Textural analysis

The mechanical properties of the different PCC batches studied were characterized by the instrumental texture method reported by Sanchez-Jimenez et al. (2022), which consisted of a hybrid flexion-compression test. A texture analyzer (TA.XT2i, Stable Micro Systems, Surrey, UK) was equipped with a spherical probe of 25 mm in diameter (P/1S, ANAME, Spain) and a hollow cylinder (50 mm external diameter) (P/50, ANAME, Spain), where the PCC was positioned. The centre of the snack was compressed up to 30 % strain at 1 mm/s with a single measurement taken per PCC, analyzing 30 samples for each batch.

The force-time curves were analyzed using the texture analyzer software (Exponent Lite®, Stable Micro System, UK) to determine the maximum force (F_{max}), which is generally adopted as an estimation of the hardness in food-textural studies. Averaged stress (σ)-strain (ε) profiles of the different batches were computed from the force-time curves and analyzed following the methodology developed and validated by Sanchez-Jimenez et al. (2022), which describes initial elastic

behaviour (Eq. (3)) followed by plastic (Eq. (4)) starting from a critical strain or yield point. The model parameters are the elastic or deformability modulus (E, MPa), the critical strain (ε_c), separating the elastic and plastic zones, and the *n* parameter, which describes the degree of concave curvature in the plastic zone. Plastic behaviour appears as a consequence of small fractures caused in the PCC during the flexion-compression test.

$$\sigma = E \cdot \varepsilon \; if \; \varepsilon \leq \varepsilon_c \quad \text{Eq. 3}$$

$$\sigma = E \cdot \varepsilon - E \cdot n(\varepsilon - \varepsilon_c)^2 if \; \varepsilon \geq \varepsilon_c \quad \text{Eq. 4}$$

The maximum of Eq. (4) represents the breaking point or failure of the PCC in the plastic zone, which occurs at ε_{max}. At this point, F_{max} is reached. Thus, the effective length of this plastic zone may be computed as the difference between ε_{max} and ε_c (Eq. (5)). An estimation of the apparent hardness (H_a, $N^{0.5}$/mm) for the PCC batch may be computed (Eq. (6)), correcting F_{max} by the PCC thickness (L, mm) and the extension of the plastic zone. L was measured from the instrumental texture test, as described by Sanchez-Jimenez et al. (2022). The use of a spherical probe allows for a better coupling with the jagged surface of the PCC, providing a more accurate estimation of its average L. In Eq. (6), the squared root of F_{max} was used due to the fact that it has previously been used for the purposes of correlation with different ultrasonic parameters (Benedito et al., 2002; Llull et al., 2002).

$$\Delta\varepsilon = \varepsilon_{max} - \varepsilon_c = \frac{1}{2n} \quad \text{Eq. 5}$$

$$H_a = \frac{\sqrt{F_{max}}}{2nL} \quad \text{Eq. 6}$$

The mathematical model (Eqs. (3) and (4)) was fitted to the average stress-strain profiles for each batch by identifying the values of the 3 model parameters that minimized the sum of the squared differences between the experimental stress and the calculated. The optimization was carried out by using the generalized reduced gradient (GRG) method by means of the Solver function of the spreadsheet Excel (Microsoft Excel 365). In order to assess the goodness of fit between the model and the experimental data, the explained variance (VAR, %, Eq. (7)), and the mean relative error (MRE, %, Eq. (8)) were computed.

$$VAR = \left(\frac{1 - S_{xy}^2}{S_y^2}\right) \cdot 100 \quad \text{Eq. 7}$$

$$MRE = \frac{\sum_{i=1}^{N} \left|\frac{\sigma_{ex} - \sigma_c}{\sigma_{ex}}\right|}{N} \cdot 100 \quad \text{Eq. 8}$$

Where S_{xy} is the standard deviation of the estimation (MPa), S_y is the standard deviation of the sample (MPa), σ_{ex} is the experimental stress (MPa), σ_c is the calculated stress (MPa) and *N* is the amount of experimental data.

2.6. Microstructural analysis

The microstructures of both the Control batch and the batches stored at 10 and 40 % RH (Set 2) were evaluated using Cryo-field emission scanning electron microscopy (Cryo-FESEM). The samples were frozen by immersion in slush nitrogen and transferred to a cryogenic unit (CT 15000 C; Oxford Instrument, Oxford, UK) where they were fractured. Afterward, the water of the samples was sublimed for 10 min and the samples were sputter coated with a thin layer of conductive platinum on top of the sample for 50 s. Finally, the samples were transferred into the FESEM (Ultra 55 FESEM, Zeiss, Oberkochen, Germany) chamber where the microstructure was observed at an accelerating voltage of 15 kV and a working distance of 15 mm. Magnifications of 200x and 500x were used to study the internal structure of the samples and the average size of air-filled cells was determined using the software Image J (National Institutes of Health, Bethesda, MD, USA).

2.7. Statistical analysis

To evaluate significant differences between the instrumental texture (E, ε_c, n parameter and H_a) and ultrasonic parameters (variation of the transmission coefficient modulus with frequency, ΔTC_f) of the batches, a one-way analysis of variance (ANOVA) was conducted. Means comparisons were performed using the Fisher Least Significant Differences (LSD) test with a 95 % confidence interval. A statistical analysis was carried out using Statgraphics Centurion XVII (Statgraphics Technologies Inc., VA, USA).

3. Results and discussion

3.1. Characterization of physicochemical properties

3.1.1. Moisture content and water activity

Commercial PCC from Set 1 presented moisture contents and a_w values ranging from 0.039 ± 0.001 to 0.045 ± 0.007 kg w/kg dm and from 0.110 ± 0.001 to 0.118 ± 0.001, respectively (Table 1). Although no significant differences ($p > 0.05$) were obtained between the moisture content and a_w of the batches from Set 1, a progressive increase in both the moisture content and a_w of the PCC in Set 2 was observed as the RH increases during storage (Table 2). Thereby, the a_w changed significantly ($p < 0.05$) from 0.119 ± 0.003 for the Control batch, to 0.341 ± 0.045 for the PCC stored at 40 %, while the moisture content increased from 0.042 ± 0.002 (Control) to 0.083 ± 0.008 (40 % RH). It is remarkable that the change in the a_w involved a mild modification of PCC's moisture content (Sanchez-Jimenez et al., 2022). This reflects the hygroscopicity of the PCC, which is directly linked to their porous structure and protein and carbohydrate-based composition (Wani &

Table 1
Commercial puffed corn cakes (Set 1). Physicochemical and ultrasonic characterizations.

	C-1	C-2	C-3	C-4	C-5	C-6	C-7
W	0.045 ± 0.007^{a}	0.040 ± 0.004^{a}	0.045 ± 0.007^{a}	0.040 ± 0.002^{a}	0.044 ± 0.001^{a}	0.044 ± 0.002^{a}	0.039 ± 0.001^{a}
a_w	0.113 ± 0.003^{a}	0.110 ± 0.001^{a}	0.115 ± 0.003^{a}	0.115 ± 0.001^{a}	0.117 ± 0.004^{a}	0.118 ± 0.001^{a}	0.115 ± 0.004^{a}
L	6.73 ± 0.70^{b}	7.27 ± 0.48^{cd}	6.84 ± 0.45^{bc}	7.69 ± 0.62^{de}	5.91 ± 0.48^{a}	7.83 ± 0.71^{e}	6.76 ± 0.61^{b}
ΔTC_f	−73.2 ± 12.8^{a}	−57.7 ± 2.6^{b}	−75.1 ± 12.9^{a}	−61.1 ± 6.9^{b}	−62.3 ± 2.6^{b}	−61.1 ± 2.6^{b}	−64.6 ± 8.1^{a}
F_{max}	12.1 ± 1.3^{c}	11.6 ± 1.6^{c}	10.9 ± 1.4^{bc}	13.7 ± 1.2^{d}	6.9 ± 1.3^{a}	11.4 ± 2.4^{c}	10.1 ± 1.7^{b}
E	1.68	1.49	1.38	1.30	0.96	1.14	1.28
ε_c	0.059	0.053	0.056	0.076	0.095	0.056	0.068
n	3.09	3.46	2.67	3.13	2.92	2.93	2.93
VAR	99.5	98.9	99.4	99.7	99.7	99.5	99.6
MRE	4.35	5.02	4.49	3.94	3.75	4.36	4.02
H_a	0.083 ± 0.004^{d}	0.068 ± 0.005^{a}	0.090 ± 0.006^{e}	0.077 ± 0.003^{bc}	0.076 ± 0.007^{b}	0.073 ± 0.007 ^{b}	0.080 ± 0.007 ^{cd}

Mean ± standard deviation (SD).
$^{a\text{-}e}$: Significant differences ($p < 0.05$).
C: Commercial puffed corn cake batch; W: moisture content (kg w/kg dm); a_w: water activity; L: thickness (mm); ΔTC_f: variation of the transmission coefficient modulus with frequency (dB/MHz); F_{max}: instrumental maximum force or hardness (N); E: deformability modulus (MPa); ε_c: critical strain; n: n parameter; VAR: variance (%); MRE: mean relative error (%) and H_a: apparent hardness ($N^{0.5}$/mm).

Table 2
Puffed corn cakes stored at different relative humidities (Set 2). Physicochemical and ultrasonic characterizations.

	Control	10 %	20 %	30 %	40 %
W	0.042 ± 0.002^{a}	0.051 ± 0.005^{b}	0.065 ± 0.008^{c}	0.076 ± 0.006^{d}	0.083 ± 0.008^{e}
a_w	0.119 ± 0.003^{a}	0.155 ± 0.018^{b}	0.218 ± 0.036^{c}	0.279 ± 0.047^{d}	0.341 ± 0.045^{e}
L	6.99 ± 0.87^{a}	7.44 ± 0.65^{b}	7.54 ± 0.69^{b}	7.56 ± 0.48^{b}	7.18 ± 0.70^{a}
ΔTC_f	−65.1 ± 9.4^{c}	−71.9 ± 15.6^{bc}	−74.4 ± 14.7^{ab}	−79.4 ± 11.4^{ab}	−81.9 ± 17.0^{a}
F_{max}	10.9 ± 2.5^{a}	13.1 ± 1.9^{b}	14.0 ± 2.8^{b}	15.7 ± 2.9^{c}	16.9 ± 2.8^{c}
E	1.25	1.34	1.24	1.22	1.31
ε_c	0.064	0.068	0.091	0.111	0.147
n	3.02	2.96	3.00	2.82	3.10
VAR	99.5	99.1	99.5	99.8	99.7
MRE	2.62	3.87	3.68	2.78	3.90
H_a	0.078 ± 0.008^{a}	0.082 ± 0.006^{b}	0.085 ± 0.006^{bc}	0.088 ± 0.006^{cd}	0.090 ± 0.007^{d}

Mean ± standard deviation (SD).
$^{a\text{-}e}$: Significant differences ($p < 0.05$).
W: moisture content (kg w/kg dm); a_w: water activity; L: thickness (mm); ΔTC_f: variation of the transmission coefficient modulus with frequency (dB/MHz); F_{max}: instrumental maximum force or hardness (N); E: deformability modulus (MPa); ε_c: critical strain; n: n parameter; VAR: variance (%); MRE: mean relative error (%) and H_a: apparent hardness ($N^{0.5}$/mm).

Kumar, 2016). Similar results were observed by Sharma (2012), who found an increase in the moisture content of rice-extruded snacks from 4 to 7 % (dry basis) after storage in controlled conditions (RH from 10 to 40 %). The experimental results show the noticeable impact of the storage conditions on the quality properties of PCC due to the close relationship between the moisture adsorption and the textural properties in this kind of product, as illustrated in the following section.

3.1.2. Textural properties

Tables 1 and 2 present the mechanical properties of both of the PCC sets. In Set 1, F_{max} ranged from 6.9 ± 1.3 to 13.7 ± 1.2 N (Table 1), pointing to significant differences ($p < 0.05$) between batches. These results indicate a high level of textural variability within the commercial batches (Fig. 3A), which was greater than that observed for moisture content and a_w (section 3.1.1), where no significant differences ($p > 0.05$) were found between batches. This variability can be partially attributed to differences in sample thickness affecting the instrumental tests, along with production factors such as corn kernel size and extrusion pressure, which influence the PCC characteristic structure and thickness. A significant linear correlation (correlation coefficient 0.813, $p < 0.05$) was found between F_{max} and the thickness, which illustrated that the thicker the sample, the higher the recorded F_{max} (Table 1). The L values reported in Table 1 represent the average and variation in PCC thickness per batch. However, the actual thickness variability is much wider due to the jagged surface, as explained in section 2.3. Hence, shape and thickness are critical factors that significantly impact instrumental texture analysis, complicating the standardization of quality control methods (Aguilera and Lillford, 2014; Peyron et al., 1997). For this reason, in the computed apparent hardness (Eq. (6)), the F_{max} was corrected by the averaged sample thickness. As for Set 2, F_{max} progressively increased as the PCC gained moisture, ranging from 10.9 ± 2.5 (Control) to 16.9 ± 2.8 N (40 % RH) (Table 2), as illustrated in the stress-strain profiles depicted in Fig. 3B. The increase in the extruded product hardness due to moisture adsorption has been reported by several authors (Sanchez-Jimenez et al., 2022; Wani and Kumar, 2016; Mazumber et al., 2007). Mazumber et al. (2007) observed extruded snacks became harder as the moisture content increased from 11 (2 % w.b.) to 39 N (10 % w.b.). Chang et al. (2000) explained the moisture-induced hardening as a result of the anti-plasticization effect of moisture, which produces greater resistance to deformation. Masavang et al. (2019) related the anti-plasticization effect in expanded cereal products with a fall in the glass transition temperature (T_g), which reflects a physical state transition leading to a denser and harder material. Therefore, the moisture adsorption affects the response of the PCC to the instrumental flexion-compression test, affecting its elastic-plastic behaviour. Thus, the hybrid flexion-compression model fits the stress-strain curves adequately in the case of Set 1 (VAR from 98.9 to 99.7 %; MRE from 3.94 to 5.02 %) and Set 2 (VAR from 99.1 to 99.8 %; MRE from 2.62 to 3.90 %), providing a satisfactory description of the viscoelastic behaviour of the PCC from both Sets (Tables 1 and 2).

In Set 1, no clear trend was observed between the identified parameters of the elastic-plastic model (Table 1) and the moisture content or the a_w. However, in Set 2, model parameters were significantly ($p < 0.05$) affected by the moisture gained. The ε_c exponentially increased from 0.064 to 0.147 as the moisture content increased from 0.042 to 0.083 kg w/kg dm (Fig. 4). The moisture gain in PCC caused a transition from a brittle to a ductile material (Mazumber et al., 2007). Ductile materials possess the capacity for the molecular rearrangement of their microscopic structure, permitting greater stress resistance (Roylance, 2001). This transition leads to an extension of the elastic zone and a delay in the appearance of plastic behaviour. Thus, the higher the ε_c,the more energy absorbed without fracture. However, the changes in the E were minimal (Table 2). Numerous authors observed a reduction in E during moisture uptake in different dry cereal products, such as crispbread (Jakubczyk et al., 2008a,b), wafers (Martínez-Navarrete et al., 2004) or corn-rye bread (Lewicki and Jakubczyk, 2004). However, those products presented a_w values above the critical a_w which determines the transition from a brittle to a ductile material, reducing the elastic modulus (Lewicki and Jakubczyk, 2004; Masavang et al., 2019). Sanchez-Jimenez et al. (2022) reported a critical a_w of over 0.5 in the analysis of PCC adsorption isotherms from 0.1 to 0.9. In the present study, the samples were under that critical a_w, which explains the

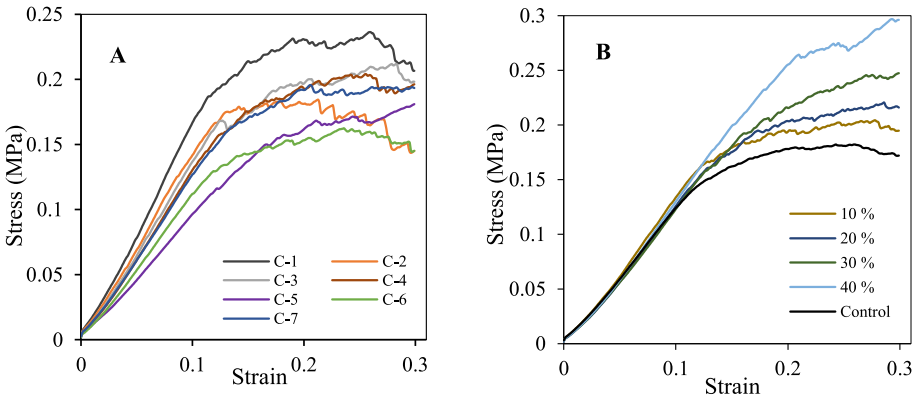

Fig. 3. A) Stress-strain profile of the commercial PCC batches (Set 1); B) stress-strain profile of the PCC batches stored at different RH between 10 and 40 % (Set 2).

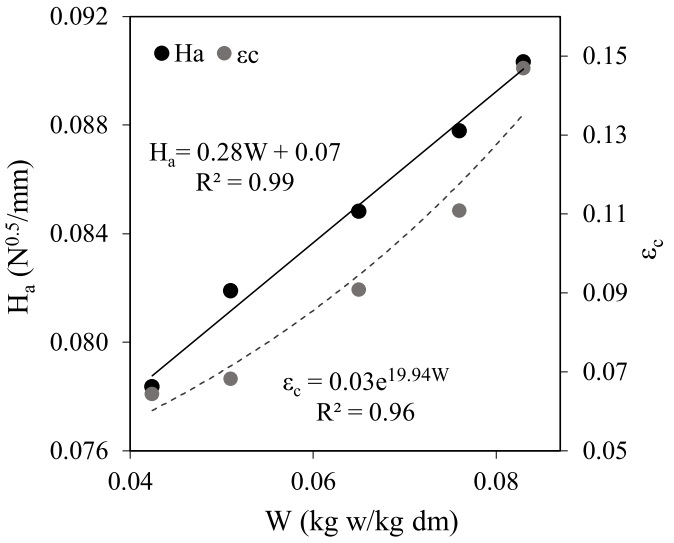

Fig. 4. Relationship between apparent hardness (H_a) and critical strain (ε_c) with moisture content (W) in PCC-Set 2. The dashed grey line represents the exponential fit of ε_c vs W and the solid black line represents the linear fit of H_a vs W.

practically constant E value (Table 2). After reaching the critical strain in the instrumental texture test, the plastic deformation of the PCC was described by the n parameter and the point of fracture, occurring at F_{max}. No clear trend in n values was identified in either set (Tables 1 and 2).

The F_{max} was corrected for the purposes of better characterizing the complex mechanical behaviour of this material; this was done by extending the plastic zone (Eq. (6)) in order to compute the apparent hardness. In Set 1, H_a values ranged from 0.068 ± 0.005 to 0.090 ± 0.006 $N^{0.5}$/mm, with significant differences ($p < 0.05$) between batches. In Set 2, the moisture gain led to a higher H_a from 0.078 ± 0.008 $N^{0.5}$/mm (Control) to 0.090 ± 0.007 $N^{0.5}$/mm (40 % RH), showing a clear linear pattern between both variables (Fig. 4, $R^2 = 0.99$). What is highlighted is the fact that there is a lower degree of inter-batch variability in H_a than in F_{max} in both sets. Specifically, H_a exhibited a variability between batches of 32 % (Set 1) and 15 % (Set 2), compared to 98.6 % (Set 1) and 55 % (Set 2) in F_{max}. The variability was defined as the difference between the maximum and minimum values within the same Set. These results underscore the significant influence of thickness on PCC hardness and suggest that H_a is a more accurate measure of PCC's mechanical properties.

3.2. Microstructural characterization

The PCC presented an internal microstructure similar to a closed-cavity solid foam, as shown in Fig. 5. This structure is based on a three-dimensional network primarily constituted by starch and proteins, forming a framework with embedded cavities (Agbisit et al., 2007; Dobraszczyk, 2008). Specifically, Fig. 5A shows the internal structure of the Control batch for Set 2, characterized by a firm and rigid matrix with cavities of defined geometry that tend to have a circular shape (Fig. 5A, orange arrow). Similar structures have been observed by different authors in cereal-extruded snacks, such as red lentil puffed snacks (Guillermic et al., 2021) and rice pellets (Zambrano et al., 2022). The internal matrix of the PCC exhibited cavities of over 35 mm in diameter with significant size variability (Fig. 5A2). This structure stems from the use of the whole corn kernel and larger extruder die during extrusion, which determines the final structure (Dobraszczyk, 2008).

Fig. 5B and C illustrate the anti-plasticizing effect of moisture adsorption on the PCC structure, stored at 10 % (0.051 kg w/kg dm) and 40 % (0.083 kg w/kg dm) RH. The alteration of the network was detected through the irregular shape and warping of the cavities, leading to the compaction and overlapping of the matrix structure (Fig. 5B2, yellow arrow). Moisture adsorption may have reduced the hydrogen bonding of the starch-protein matrix characteristic of dry-cereal snacks, increasing molecular mobility, reducing the rigidity of the solid structure (Katz and Labuza, 1981; Li et al., 2019) and, finally, making the material less sensitive to micro-fractures. In contrast, the well-defined cavities (Fig. 5A, orange arrow) observed in the control sample, were less prominent in Fig. 5B and C. This suggests the densification of the material during moisture adsorption. Thus, when there was a void size reduction from 35 mm (Control) to 6.2 mm (40 %), the structure was observed to swell and the cavities to shrink. However, there is still limited knowledge as regards the effect of moisture adsorption during storage on the microstructure of cereal snacks. Literature has mainly focused on the effect of moisture content during extrusion. For example, Sharifi et al. (2021) observed an increase in cavity wall thickness (from 17.5 to 50 μm) in puffed corn snacks after extrusion, as the moisture content increased from 15 to 18 % (d.b.). In addition, Lazou & Krokida (2010) described a thickening of the cavity walls and an increase in the void size of lentil extruded snacks as the moisture content increased from 13 to 19 % (w.b.). Both studies linked the increase in moisture content to a negative impact on product quality, leading to a texture that is denser, less crispy and harder. The anti-plasticizing effect was related to a partial plasticization of the air cell wall material, increasing cohesion and the toughness of the product structure (Masavang et al., 2019).

3.3. Ultrasonic testing

The typical frequency-decay of the transmission coefficient with the frequency is illustrated in Fig. 2B. In the frequency range analyzed, the experimental data (TC vs. Frequency) followed a linear distribution and its slope (ΔTC_f) can be used as an estimation of the material attenuation. Attenuation is related to the absorption, scattering and reflection of the US waves through the PCC (Ginel and Alvarez-Arenas, 2019). In the case of PCC, the high air content and the heterogeneous and multiphase structure of this material (Fig. 5A) contribute to US attenuation (Kerhervé et al., 2019; Koksel et al., 2016a; Scanlon and Page, 2015). Koksel et al. (2016b) reported that multi-phase material presented a density difference between the air-solid interfaces, leading to scattering phenomena. In Set 1 (Table 1), ΔTC_f ranged from −75.1 ± 12.9 (batch C-3) to −57.7 ± 2.6 dB/MHz (batch C-2). Although neither the moisture content nor the water activity was found to exert a significant ($p > 0.05$) influence on ΔTC_f, due to the narrow experimental range for W and a_w, significant differences ($p < 0.05$) in the average ΔTC_f were found between batches (Table 1). The variations in the ultrasonic parameter observed in Set 1 may be related to the different production factors (pressure, kernel die, corn grain dimensions, etc.) mentioned above (Section 3.1.2). These factors could produce variations in PCC structure, which would affect ultrasonic propagation. Therefore, the ΔTC_f could be linked to PCC textural properties, as will be explained in Section 3.4.

3.3.1. Influence of moisture content on ultrasonic parameters

Fig. 6 shows the effect of increasing PCC moisture content on ΔTC_f, leading to a progressive reduction in the attenuation-related ultrasonic parameter for Set 2. The ΔTC_f values for the Control and 40 % batches ranged from −65.1 ± 9.4 (0.042 kg w/kg dm) to −81.9 ± 17.0 dB/MHz (0.083 kg w/kg dm), respectively. Thus, the ΔTC_f variability was slightly greater for Set 2 compared to Set 1, indicating that manufacturing processes may lead to significant modifications in the PCC texture, similar to those associated with minor moisture increases. Due to the negative sign, a reduction in ΔTC_f entails a larger attenuation. A linear pattern ($R^2 = 0.96$) was found between the ΔTC_f and the moisture content of Set 2 (Fig. 6). Thus, the modification of the PCC's structure due to moisture gain (Fig. 5) affected wave transmission, leading to increased attenuation. The influence of the moisture content on US-related parameters has been analyzed in the literature, with the observed effects being product-dependent (Elmehdi, 2020; Scanlon and

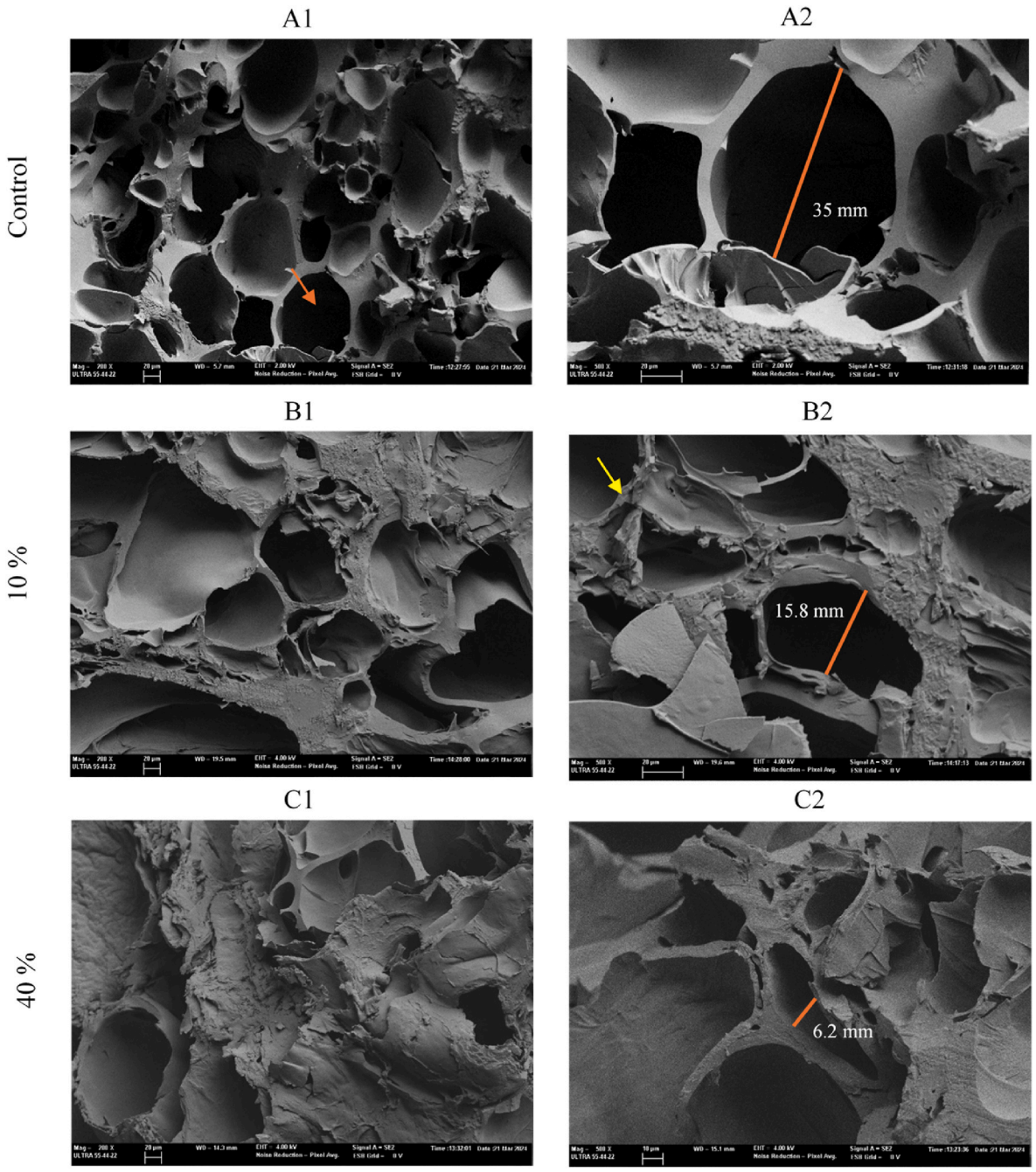

Fig. 5. Internal microstructure of puffed corn cakes (PCC) by means of Cryo-field emission scanning electron microscopy: A) Control batch; B) moisture adsorption at 10 % RH and C) batches at 40 % RH. Orange arrow: void cavity; yellow arrow: solid-matrix overlapping and orange lines: void size (mm). Magnification: 200× (1) and 500x (2). (For interpretation of the references to colour in this figure legend, the reader is referred to the Web version of this article.)

Page, 2015). Kerhervé et al. (2019) reported higher attenuation coefficient values in noodle dough samples at a high (38 % w.b.) moisture content than at low (34 % w.b.). Sanchez-Jimenez et al. (2023) obtained similar results in potato drying, in which a more intense attenuation was found for the raw material (−205 dB/MHz at 3.80 kg w/kg dm) than the dried (−55 dB/MHz at 0.11 kg w/kg dm). The attenuation changes shown by these authors could be linked to a transition state of the food matrices due to the increase or reduction in the moisture content. Moisture adsorption leads to a less brittle and more ductile material, making it more deformable. This means that under the action of the ultrasonic wave, the deformation and molecular rearrangement can be bigger, leading to greater internal friction that will contribute to an increase in the attenuation of the ultrasonic wave. In the case of PCC, it was possible to observe appreciable changes in the solid-matrix structure, tending towards a size reduction of the closed cavities and a densification of the matrix as a result of moisture gain (Section 3.2). Despite extensive research into the effect of water adsorption on the viscoelastic properties of extruded cereal snacks, to our knowledge, this study has addressed the ultrasonic testing of this kind of product for the first time. This may be explained by the fact that the analysis of this type of product cannot be addressed using conventional approaches (direct-contact sensors). The jagged surface prevents good coupling with the sensor, and the use of coupling materials (gels or water) is totally undesirable.

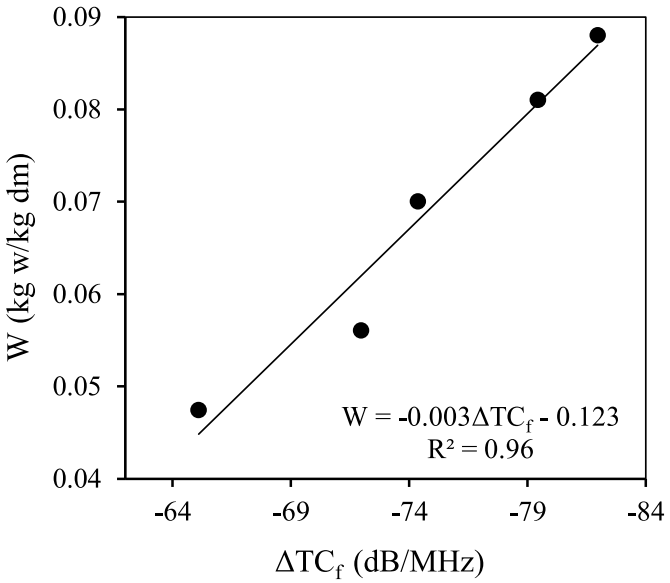

Fig. 6. Relationship between the variation in the transmission coefficient modulus with frequency (ΔCT_f) and the moisture content (W) of PCC-Set 2. The black line represents the linear fit.

3.4. Characterization of textural properties

Fig. 7 shows the relationship between the ultrasonic (ΔTC_f) and textural (H_a and ε_c) parameters. A satisfactory linear fit ($R^2 = 0.89$) was found between ΔTC_f and H_a for both PCC Sets (Fig. 7A). Thereby, the ΔTC_f parameter was able to describe the mechanical response of PCC batches both from Set 1, which was mainly influenced by production factors, and from Set 2, which was linked to moisture changes during storage. The increase in H_a may be due to the anti-plasticizing effect on the PCC structure caused by the moisture gain. This moisture converts a rigid network with well-defined cavities into a more compact matrix with warped cavities (sections 3.1.2 and 3.2), leading to increased hardness and a longer plastic period before reaching the breaking point. In every case, the higher the H_a of the PCC, the lower the ΔTC_f, which entails greater attenuation.

For Set 2, an exponential relationship ($R^2 = 0.88$) was found between ε_c and ΔTC_f (Fig. 7B), based on the aforementioned relationship between the ε_c and the moisture content (Fig. 4). In this context, the increase in ε_c leads to lower ΔTC_f, which could be associated with the transition of PCC from brittle to ductile, as previously explained (Section 3.1.2). This structural modification leads to a higher degree of attenuation by scattering, absorption or by a combination of both. Hence, the commercial (Set 1) and Control (Set 2) batches that were not moisturized were primarily influenced by the combination of scattering and absorption, which was the main source of the ultrasonic energy loss due to their internal structure having air cavities. In contrast, the attenuation of PCC after moisture gain (Set 2) could be mainly controlled by absorption, owing to the compaction of the matrix and the transition of the state of the material, resulting in increased attenuation. Thus, previous studies have linked the more predominant role of plastic behaviour in food matrices to greater ultrasonic attenuation (Fariñas et al., 2021a; Povey and Hefft, 2023). However, to our knowledge, no previous studies have addressed the viscoelastic properties of extruded cereal-based products through a contactless ultrasonic technique.

4. Conclusions

This study has illustrated the feasibility of the air-coupled ultrasound technique to characterize the textural properties of puffed corn cakes (PCC). The textural traits of PCC exhibit a high degree of variability due to their ingredients and manufacturing conditions, which hinder the standardization of structure and thickness during production. An attenuation-related ultrasonic parameter has been identified as a promising indicator for the description of the textural properties of PCC. This parameter, derived from the slope of the transmission coefficient with frequency (ΔTC_f), is not dependent on sample thickness, unlike textural properties estimated from instrumental tests. Furthermore, the study highlights the potential of ΔTC_f to predict the increases in moisture content resulting from exposure to relative humidity during storage or production, which in turn affects the final texture of PCC. The increase in attenuation in PCC with a greater moisture content was linked with microstructural compaction and overlapping air cavities from the internal PCC matrix. These results highlight significant progress in the digitalization of the industry (Industry 4.0). The contactless ultrasonic technique enables rapid, real-time, and completely non-invasive quality control of extruded cereal snacks by measuring the entire production process. However, further efforts are needed to assess the feasibility of air-coupled ultrasound in an industrial environment and explore its integration with data science techniques to effectively manage the information generated by ultrasonic sensors.

CRediT authorship contribution statement

Virginia Sanchez-Jimenez: Writing – original draft, Methodology, Investigation, Formal analysis. **Lola Fariñas:** Writing – original draft, Methodology, Investigation, Formal analysis. **Anabella S. Giacomozzi:** Writing – review & editing, Formal analysis. **Alba Ginel:** Investigation. **Amparo Quiles-Chuliá:** Writing – review & editing, Investigation. **Tomas E. Gomez Alvarez-Arenas:** Writing – review & editing, Project administration, Methodology, Funding acquisition, Formal analysis,

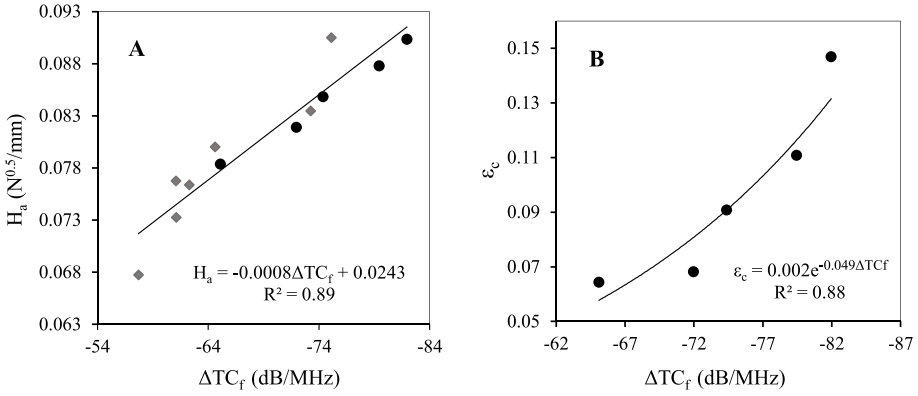

Fig. 7. Relationship between the variation of the transmission coefficient modulus with frequency (ΔCT_f) with A) apparent hardness (H_a) of PCC (Set 1 grey diamonds, Set 2 black dots) and B) the critical strain of PCC-Set 2. The black line represents the linear and exponential fit in A and B, respectively.

Conceptualization. **Jose Benedito:** Writing – review & editing, Project administration, Funding acquisition, Formal analysis. **Jose V. Garcia-Perez:** Writing – review & editing, Supervision, Project administration, Funding acquisition, Formal analysis, Conceptualization.

Declaration of competing interest

None.

Acknowledgements

The authors acknowledge the financial support through the projects ULTRADIGITAL (AGROALNEXT/2022/045), which is part of the AGROALNEXT programme, supported by MCIN with funding from the European Union NextGenerationEU (PRTR-C17.I1) and by Generalitat Valenciana and the Projects RTC-2017-6314-2,3 funded by "Ministerio de Ciencia, Innovación y Universidades" and "Agencia Estatal de Investigación" in Spain. The authors deeply acknowledge the support in this investigation from Cerealto Group.

Nomenclature

PCC	Puffed corn cakes
N	Number of the experimental data
RH	Relative humidity, %
W	Moisture content, kg water (w)/kg dry matter (dm)
a_w	Water activity
TOF	Time-of-flight, s
FFT	Fast Fourier Transform
TC	Transmission coefficient spectra
ΔTC_f	Variation of the transmission coefficient modulus with frequency, dB/MHz
A	Amplitude of each frequency of PCC spectrum
A_0	Amplitude of reference signal
F_{max}	Maximum force or hardness, N
E	Elastic or deformability modulus, MPa
σ	Stress, MPa
ε	Strain
n	Parameter in Eq. 4
ε_c	Critical strain
ε_{max}	Maximum strain
H_a	Apparent hardness, $N^{0.5}$/mm
L	Thickness, mm
GRG	Generalized reduced gradient method
sd	Standard deviation
VAR	Explained variance, %
MRE	Mean relative error, %
S_{xy}	Standard deviation of the estimation
S_y	Standard deviation of the sample
σ_{ex}	Experimental stress, MPa
σ_c	Calculated stress, MPa
d.b.	Dry basis
w.b.	Wet basis
R^2	Coefficient of determination

Data availability

Data will be made available on request.

References

Agbisit, R., Alavi, S., Cheng, E., Herald, T., Trater, A., 2007. Relationships between microstructure and mechanical properties OF cellular cornstarch extrudates. J. Texture Stud. 38, 199–219.

Aguilera, J.M., Lillford, P.J. (Eds.), 2014. Food Materials Science. Principles and Practice. https://doi.org/10.1007/978-1-4471-6377-0_10.

Awad, T.S., Moharram, H.A., Shaltout, O.E., Asker, D., Youssef, M.M., 2012. Applications of ultrasound in analysis, processing and quality control of food: a review. Food Res. Int. 48, 410–427. https://doi.org/10.1016/j.foodres.2012.05.004.

Benedito, J., Carcel, J.A., Gonzalez, R., Mulet, A., 2002. Application of low intensity ultrasonics to cheese manufacturing processes. Ultrasonics 40, 19–23. https://doi.org/10.1016/S0041-624X(02)00085-9.

Chang, Y.P., Cheah, P.B., Seow, C.C., 2000. Variations in flexural and compressive fracture behavior of a brittle cellular food (dried bread) in response to moisture sorption. J. Texture Stud. 31, 525–540. https://doi.org/10.1111/j.1745-4603.2000.tb01018.x.

Contreras, M., Benedito, J., Garcia-Perez, J.V., 2021. Ultrasonic characterization of salt, moisture and texture modifications in dry-cured ham during post-salting. Meat Sci. 172. https://doi.org/10.1016/j.meatsci.2020.108356.

Dobraszczyk, B.J., 2008. Structured cereal products. In: Food Material Science, pp. 475–500.

Elfawakhry, H., Hussein, M.A., Becker, T., 2013. Investigations on the evaluation of rheological properties of cereal based viscoelastic fluids using ultrasound. J. Food Eng. 116, 404–412. https://doi.org/10.1016/j.jfoodeng.2012.12.021.

Elmehdi, H.M., 2020. A novel nondestructive ultrasonic velocity and attenuation approach for sustainable quality prediction of wheat-based products. In: Advances in Science, Technology and Innovation, pp. 1–7.

Fariñas, L., Contreras, M., Sanchez-Jimenez, V., Benedito, J., Garcia-Perez, J.V., 2021a. Use of air-coupled ultrasound for the non-invasive characterization of the textural properties of pork burger patties. J. Food Eng. 297. https://doi.org/10.1016/j.jfoodeng.2021.110481.

Fariñas, L., Sanchez-Torres, E., Sanchez-Jimenez, V., Diaz, R., Benedito, J., Garcia-Perez, J.V., 2021b. Assessment of avocado textural changes during ripening by using contactless air-coupled ultrasound. J. Food Eng. 289. https://doi.org/10.1016/j.jfoodeng.2020.110266.

Gan, T.H., Hutchins, D.A., Billson, D.R., 2002. Preliminary studies of a novel air-coupled ultrasonic inspection system for food containers. J. Food Eng. 53, 315–323. https://doi.org/10.1016/S0260-8774(01)00172-8.

Gan, T.H., Pallav, P., Hutchins, D.A., 2006. Non-contact ultrasonic quality measurements of food products. J. Food Eng. 77, 239–247. https://doi.org/10.1016/j.jfoodeng.2005.06.026.

Ginel, A.M., Alvarez-Arenas, T.G., 2019. Air-coupled transducers for quality control in the food industry. In: IEEE International Ultrasonics Symposium, IUS 2019-Octob, pp. 803–806. https://doi.org/10.1109/ULTSYM.2019.8925853.

González-Mohino, A., Jiménez, A., Paniagua, M.J., Perez-Palacios, T., Rufo, M., 2019. New contributions of ultrasound inspection to the characterization of different varieties of honey. Ultrasonics 96, 83–89. https://doi.org/10.1016/j.ultras.2019.02.010.

Guillermic, R.M., Aksoy, E.C., Aritan, S., Erkinbaev, C., Paliwal, J., Koksel, F., 2021. X-Ray microtomography imaging of red lentil puffed snacks: processing conditions, microstructure and texture. Food Res. Int. 140, 109996. https://doi.org/10.1016/j.foodres.2020.109996.

Hassoun, A., Jagtap, S., Garcia-Garcia, G., Trollman, H., Pateiro, M., Lorenzo, J.M., Trif, M., Rusu, A.V., Aadil, R.M., Šimat, V., Cropotova, J., Câmara, J.S., 2023. Food quality 4.0: from traditional approaches to digitalized automated analysis. J. Food Eng. 337. https://doi.org/10.1016/j.jfoodeng.2022.111216.

Jakubczyk, E., Marzec, A., Lewicki, P.P., 2008a. Relationship between water activity of crisp bread and its mechanical properties and structure. Pol. J. Food Nutr. Sci. 58, 45–51.

Jakubczyk, E., Marzec, A., Lewicki, P.P., 2008b. Relationship between water activity of crisp bread and its mechanical properties and structure. Pol. J. Food Nutr. Sci. 58, 45–51.

Jiang, Z., Wang, K., Zhao, X., Li, J., Yu, R., Fu, R., He, Y., Zhao, P., Oh, K.C., Hou, J., 2021. High-protein nutrition bars: hardening mechanisms and anti-hardening methods during storage. Food Control 127. https://doi.org/10.1016/j.foodcont.2021.108127.

Katz, E.E., Labuza, T.P., 1981. Effect of water activity on the sensory crispness and mechanical deformation of snack food products. J. Food Sci. 46, 403–409. https://doi.org/10.1111/j.1365-2621.1981.tb04871.x.

Kelly, S.P., Hayward, G., Gomez, T.E., 2001. AN air-coupled ultrasonic matching layer employing half wavelength cavity resonance. Ultrasonics 965–968.

Kerhervé, S.O., Guillermic, R.M., Strybulevych, A., Hatcher, D.W., Scanlon, M.G., Page, J.H., 2019. Online non-contact quality control of noodle dough using ultrasound. Food Control 104, 349–357. https://doi.org/10.1016/j.foodcont.2019.04.024.

Koksel, F., Scanlon, M.G., Page, J.H., 2016a. Ultrasound as a tool to study bubbles in dough and dough mechanical properties: a review. Food Res. Int. 89, 74–89. https://doi.org/10.1016/j.foodres.2016.09.015.

Koksel, F., Scanlon, M.G., Page, J.H., 2016b. Ultrasound as a tool to study bubbles in dough and dough mechanical properties: a review. Food Res. Int. 89, 74–89. https://doi.org/10.1016/j.foodres.2016.09.015.

Laurindo, J.B., Peleg, M., 2007. Mechanical measurements in puffed rice cakes. J. Texture Stud. 38, 619–634. https://doi.org/10.1111/j.1745-4603.2007.00116.x.

Lazou, A., Krokida, M., 2010. Structural and textural characterization of corn-lentil extruded snacks. J. Food Eng. 100, 392–408. https://doi.org/10.1016/j.jfoodeng.2010.04.024.

Lewicki, P., Jakubczyk, E., 2004. Effect of water activity on mechanical properties of dry cereal products. Acta Agrophysica 4, 381–391.

Li, R., Lin, D., Roos, Y.H., Miao, S., 2019. Glass transition, structural relaxation and stability of spray-dried amorphous food solids: a review. Dry. Technol. 37, 287–300. https://doi.org/10.1080/07373937.2018.1459680.

Llull, P., Simal, S., Benedito, J., Rosselló, C., 2002. Evaluation of textural properties of a meat-based product (sobrassada) using ultrasonic techniques. J. Food Eng. 53, 279–285. https://doi.org/10.1016/S0260-8774(01)00166-2.

Martínez-Navarrete, N., Moraga, G., Talens, P., Chiralt, A., 2004. Water sorption and the plasticization effect in wafers. Int. J. Food Sci. Technol. 39, 555–562. https://doi.org/10.1111/j.1365-2621.2004.00815.x.

Masavang, S., Roudaut, G., Champion, D., 2019. Identification of complex glass transition phenomena by DSC in expanded cereal-based food extrudates: impact of plasticization by water and sucrose. J. Food Eng. 245, 43–52. https://doi.org/10.1016/j.jfoodeng.2018.10.008.

Mohd Khairi, M.T., Ibrahim, S., Md Yunus, M.A., Faramarzi, M., 2016. Contact and non-contact ultrasonic measurement in the food industry: a review. Meas. Sci. Technol. 27. https://doi.org/10.1088/0957-0233/27/1/012001.

Morrison, D.S., Abeyratne, U.R., 2014. Ultrasonic technique for non-destructive quality evaluation of oranges. J. Food Eng. 141, 107–112. https://doi.org/10.1016/j.jfoodeng.2014.05.018.

Peyron, M.A., Maskawi, K., Woda, A., Tanguay, R., Lund, J.P., 1997. Effects of food texture and sample thickness on mandibular movement and hardness assessment during biting in man. J. Dent. Res. 76, 789–795. https://doi.org/10.1177/00220345970760031201.

Roylance, D., 2001. Stress-strain curves. Aluminum alloy castings 193–209. https://doi.org/10.31399/asm.tb.aacppa.t51140193.

Sanchez-Jimenez, V., Collazos-Escobar, G.A., Gonz, A., Alvarez-Arenas, E.G., Benedito, J., Garcia-Perez, J.V., 2023. Non-invasive Monitoring of Potato Drying by Means of Air-Coupled Ultrasound, vol. 148, pp. 0–9. https://doi.org/10.1016/j.foodcont.2023.109653.

Sanchez-Jimenez, V., Gomez Alvarez-Arenas, T.E., Rincón, M., Benedito, J., Garcia-Perez, J.V., 2022. Assessment of textural properties of puffed corn cakes during storage at different relative humidity. Foods 11. https://doi.org/10.3390/foods11182882.

Scanlon, M.G., Page, J.H., 2015. Probing the properties of dough with low-intensity ultrasound. Cereal Chem. 92, 121–133. https://doi.org/10.1094/CCHEM-11-13-0244-IA.

Sharifi, S., Majzoobi, M., Farahnaky, A., 2021. Effects of particle size and moisture content of maize grits on physical properties of expanded snacks. J. Texture Stud. 52, 110–123. https://doi.org/10.1111/jtxs.12565.

Sharma, J.K., 2012. The Structure and Properties of Puffed Rice Cakes. B.Sc Science Punjab Agricultural University.

Strybulevych, A., Diep, S., Daugelaite, D., Guillermic, R.M., Page, J.H., Hatcher, D.W., Scanlon, M.G., 2019. Velocity and attenuation analysis methods for characterizing the properties of wheat flour noodle dough. Cereal Chem. 96, 647–654. https://doi.org/10.1002/cche.10160.

Vasighi-Shojae, H., Gholami-Parashkouhi, M., Mohammadzamani, D., Soheili, A., 2018. Ultrasonic based determination of apple quality as a nondestructive technology. Sens. Bio-Sens. Res. 21, 22–26. https://doi.org/10.1016/j.sbsr.2018.09.002.

Wani, S.A., Kumar, P., 2016. Moisture sorption isotherms and evaluation of quality changes in extruded snacks during storage. LWT - Food Sci. Technol. (Lebensmittel-Wissenschaft -Technol.) 74, 448–455. https://doi.org/10.1016/j.lwt.2016.08.005.

Zambrano, Y., Contardo, I., Moreno, M.C., Bouchon, P., 2022. Effect of extrusion temperature and feed moisture content on the microstructural properties of rice-flour pellets and their impact on the expanded product. Foods 11. https://doi.org/10.3390/foods11020198.